Vulnerability and Retrofitting of Torsionally Deformable RC buildings: a case study

Maria Gabriella Mulas[1], *Lorenzo Stroffolini*[1], *Paolo Martinelli*[1*]

[1]Department of Civil and Environmental Engineering, Politecnico di Milano, Milan, Italy

[*]Corresponding author. E-mail: paolo.martinelli@polimi.it

ABSTRACT: The paper presents the seismic vulnerability assessment and the subsequent retrofitting strategies of a reinforced concrete (RC) strategic building in Italy. At time of design, the erection site was not classified as a seismic area. With a structural layout widely spread in non-seismic zones and for buildings designed with obsolete seismic codes, the framed system was designed for gravity loads only, with an eccentric lift core and moment-resisting frames aligned in one direction. The structural seismic capacity is impaired by torsional deformability and the possible appearance of both brittle collapse mechanisms and pounding phenomena with an adjacent building, while the seismic demand is governed by the classification of "strategic building". Two retrofitting strategies are here analysed, under the constraints of eliminating the torsional deformability and minimizing the interruption of normal activities in the building. The results highlight the advantages and disadvantages of the two strategies and the most important features of the structural response, providing indications for further actions. The adoption of a design spectrum reduced by a 0.6 factor, roughly equivalent to that for an ordinary building, extends the relevance of the work well beyond the case study.

KEYWORDS: *RC non-ductile frame, torsional deformability, seismic vulnerability, obsolete codes, retrofitting strategies, strategic building.*

1 Introduction

The recent earthquakes in L'Aquila (2009) and on the Po Plain (2012) brought to light different aspects of the vulnerability of the Italian civil and industrial building stock. In the town of L'Aquila, the collapse of ten reinforced concrete (RC) buildings resulted in about half of the casualties, but the large majority of buildings of the same class and age (built in the '50-60'), while suffering severe damage survived the earthquake, guaranteeing the primary function of saving life. The damage of the Po Plain event concerned mainly industrial precast buildings, erected without enforcing seismic prescriptions. In both cases, damage can be attributed to inadequacy of Technical Codes. Obsolete seismic codes, based on a limited knowledge, and delay both in encompassing recent knowledge and in seismic zonation, are the most common causes of the vulnerability of buildings.

For RC buildings having a rectangular plan, a widely spread structural scheme is composed of a parallel moment resisting frame aligned in the longitudinal direction and floor systems in the transverse direction. This resisting scheme, very effective in carrying gravity loads, lacks in bi-directionality and results in buildings characterized

by a strong and a weak direction, the former being that of the frames and the latter the perpendicular one (Mulas et al 2013; Mulas & Martinelli, 2017). Thus, the adequacy of their seismic behaviour is not guaranteed, if they are located in an area that today is classified to be of moderate or high seismicity. The extension to the entire Italy of the seismic zonation was only made in 2003 (OPCM 3274, 2003). In 2008, in the framework of performance-based design, a new technical code (NTC 2008, 2008) defined multiple performance objectives (Figure 1), in which a level of performance, expressed in terms of damage state, is associated to a hazard level, in terms of exceedance probability P_{VR} in the reference period $V_{R,}$ that describes the expected seismic load at site (Kunnath, 2005).

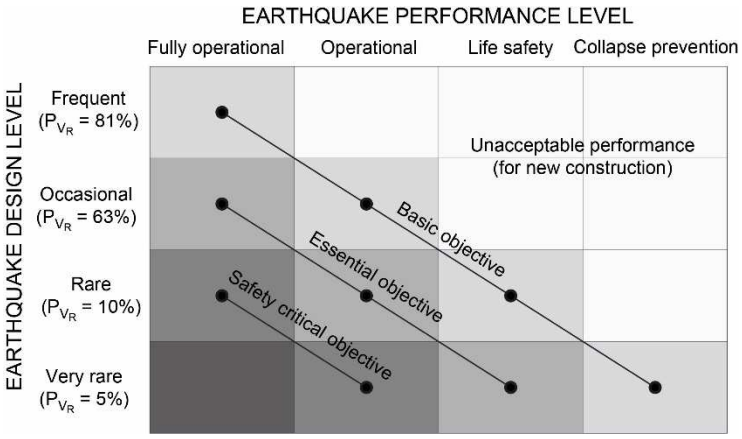

Figure 1 – Performance objectives (Kunnath 2005).

Nowadays, diagnostics and subsequent planning of retrofitting interventions make it possible to reduce seismic vulnerability. The literature reports several examples of strengthening techniques for non-ductile RC structures (Thermou and Elnashai, 2006; Thermou et al., 2012; Thermou and Psaltakis, 2018; Zerbin and Aprile, 2015; Mazza, 2015). Moreover, over the past two decades, a large number of studies were conducted on Fibre Reinforced Polymer (FRP) wrapping (among the others Ilki et al., 2012; Del Zoppo et al. 2017) and steel jacketing techniques (e.g. Xiao and Wu, 2003; Choi et al., 2010) used to retrofit and to strengthen the existing RC columns. A detailed review of conventional repair schemes for RC frame buildings was reported by Thermou and Elnashai, (2006). Local (i.e., injection of cracks, shotcrete, steel plate adhesion, steel jacketing, externally bonded FRPs) as well as global (i.e., RC jacketing, addition of walls, external buttresses, steel bracing, base isolation) strengthening measures were discussed and their technological application details outlined. Although a multiplicity of factors influence the selection of the retrofit solution, Thermou and Elnashai (2006) proposed a table summary of the retrofit options, motivation for use, local and global effects, technological and design requirements, intended to provide a rapid guide to potential users. A review of the possible alternative choices for retrofitting and possible criteria for the mitigation of seismic risk is also presented by Calvi (2013). It is shown that it is possible to associate a loss analysis to different strengthening strategies, depending on the cost of intervention. A design methodology

for the seismic upgrading of torsionally sensitive substandard RC buildings was proposed by Thermou and Psaltakis (2018). The methodology aims firstly to eliminate the effect of torsional coupling on modal properties through the addition of peripheral RC walls and then to modify the lateral response shape of the building in each direction, to achieve an optimum distribution of interstory drift along the building height. Zerbin and Aprile (2015) presented four different design solutions for the retrofit of an existing RC frame with poor concrete quality and inadequate reinforcement detailing. Strengthening solutions are based on FRP wrapping of the existing structural elements or alternatively on the introduction of new RC shear walls. They concluded that low cost and non-invasive FRP wrapping is in general the best solution to retrofit existing RC buildings.

The choice of retrofitting techniques should take into account geometric limitations, architectural constraints and both economic and operational feasibility considerations, as well as the possible interruption of the normal activities, if an invasive intervention is planned. Problems arise when retrofitting is applied to structures whose load histories are not completely known, the availability of the original design documents and drawings is limited, and it is difficult to accurately access the state of damage and degradation of concrete and steel.

Within the building stock, the assessment of seismic vulnerability of strategic facilities, such as hospital and school buildings, is of paramount importance to guarantee functionality even under extreme conditions. For the reasons pointed out previously, a large number of strategic buildings was designed without adequate seismic criteria. Recent studies showed the pronounced fragility and vulnerability of Italian strategic buildings under seismic actions (Perrone et al. 2015; Ruggieri et al. 2020; Ruggieri et al. 2021). Perrone at al. (2015) proposed a Rapid Visual Screening (RVS) method to determine a Safety Index for hospital buildings. The method includes the influence of hazard and exposure and focused on the peculiarities of Italian hospital buildings including the vulnerability of structural and non-structural elements. The procedure was applied to two Italian RC hospital buildings built in the same period but in areas with different seismic risks. High and medium levels of risks were identified for them: the absence of seismic detailing and the irregularity of the structure played an important role in classifying one of the two in a high level of risk. In their study Ruggieri et al. (2020) proposed a RVS procedure for the seismic risk assessment of RC school buildings. The methodology, which accounts for the characteristics of Italian RC school buildings, includes both exposure and hazard in the evaluation of the Safety Index. The RVS methodology was applied to ten RC school buildings and the results showed that most of the buildings had structural deficiencies due to in-plan and in-elevation irregularities as well as to the absence of structural detailing.

The aim of this paper is to study the vulnerability and to discuss the retrofitting strategies for a rectangular building with unidirectional frames and eccentric cores. The case study belongs to a RC strategic construction located in Italy, designed for gravity and wind loads only. The erection site was not included in the areas of seismic risk in

the zonation of Italian seismic codes, and had not been struck by any strong earthquake since the building construction. Nowadays, the status of "*strategic building*" is associated to a very high seismic risk (see Figure 1), that must be tackled by a structure that was correctly designed for gravity loads but not to provide a satisfactory seismic behaviour, whose design documents are not completely available. In addition, the building functionality should be guaranteed during retrofitting operations and floor plans cannot be modified, limiting the insertion of new elements to the building perimeter. All these issues are discussed in the paper. For confidentiality reasons, extensive details about the overall geometry and location of the construction cannot be provided.

In the following, Section 2 describes the structure. Section 3 is devoted to structural modelling. The assessment of seismic vulnerability is addressed, through both linear and nonlinear analyses, in Section 4. Section 5 presents a few options for retrofitting strategies; whose results are discussed in Section 6. Conclusions are drawn in Section 7. The Italian Code prescriptions adopted in this work (NTC 2018, 2018; Circolare n. 7, 2019), are similar or equal to those of Eurocode 8 (EN 1998-1, 2005; EN 1998-3, 2005). Notable differences will be highlighted within the text.

2 The Building under Study

The strategic building under study is composed of many adjacent buildings, having independent RC framed structures for vertical loads bearing capacity, separated by joints. This study considers only two of them, which are precast buildings erected at the beginning of the 90's and depicted in Figure 2. Building B1 is analysed in detail, while only dynamic properties are determined for Building B2, to evaluate pounding phenomena between them. In this respect, it must be taken into account that seismic interaction between adjacent buildings that are partly and in a non-symmetric way in contact may introduce significant torsional oscillations (Karayannis and Naoum, 2018). This type of structural interaction, referred to as asymmetric pounding, is unlikely in the buildings under investigation, having both the same story heights and the same story levels. Hence, their potential interaction can be classified as a diaphragm-to-diaphragm collision, typically less severe than a diaphragm-to-column collision, taking place when the story levels of the two structures are different.

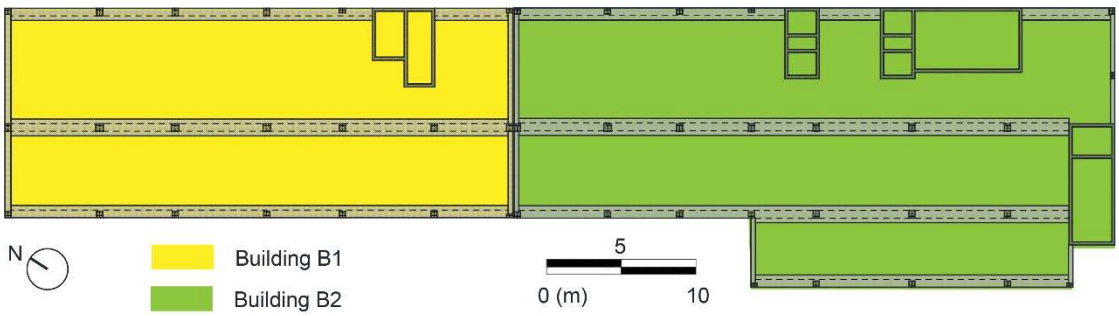

Figure 2 - Plan of Buildings B1 (the case study) and B2. Stairs are located in B2 only.

Available design documents include neither architectural drawings, here deduced from safety plans, nor vertical cross-sections. Technical drawings are available for slabs, but not for precast columns and beams. A design document named “Table of Columns” provides, at each story, cross-section dimensions and reinforcement geometry for all the columns. For beams, the outputs of a commercial code are the only source of relevant data. Due to the lack of on-site tests, in this work a numerical simulation of the initial design provided a partial validation of reinforcement geometry. Foundation plans do not include the details of the reinforcement geometry. Design loads and property of materials for precast elements can be deduced from technical reports. Tests certificates are available for cast-in-situ concrete only. A limited uncertainty also affects the steel properties.

2.1 The structural system

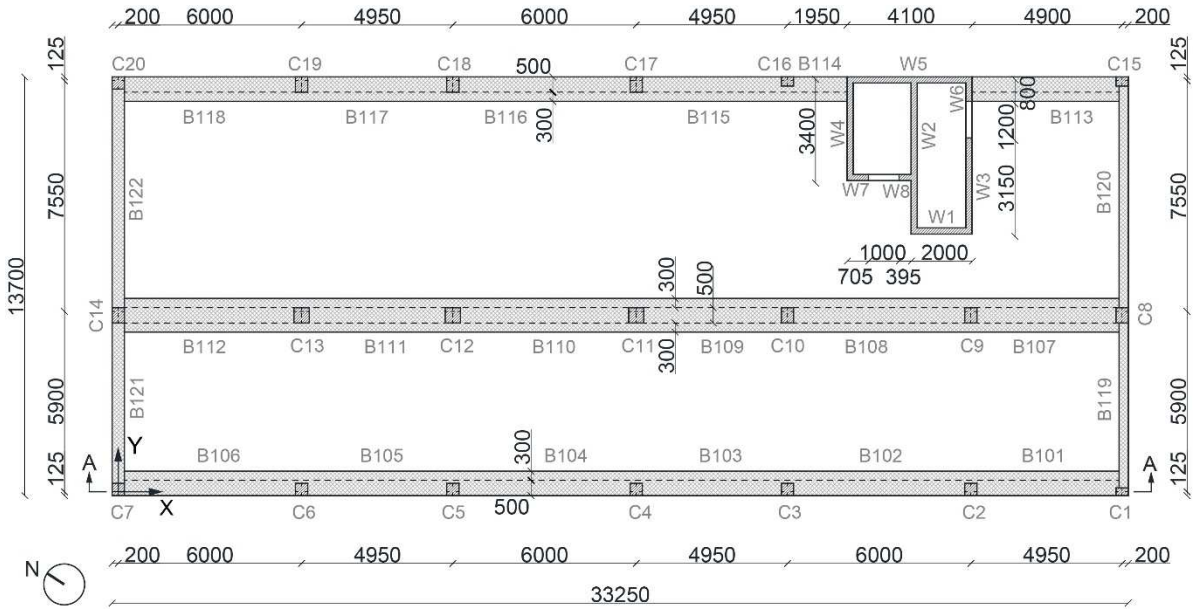

Figure 3 – Building B1, ground floor plan, with the elevator core (left) and the technical core (right). Units: mm; columns, beams and wall numbers in grey.

The 4-story Building B1 cannot be classified as regular in plan according to NTC 2018 (2018), due to the lack of symmetry about two perpendicular axes. At the building top, a horizontal roof supports a technical compartment for the elevator machinery. Floors have a rectangular configuration of 33.25×13.7 m. Figure 3 shows the plan view of the first/typical floor, while Figure 4 shows a longitudinal section. The short side (Y-direction) of the building is divided into two spans, 5.9 m and 7.55 m long, while 6 bays span along the X-direction, alternatively 6 m or 4.95 m long. The resisting system of Building B1 is composed of three parallel frames acting along the longitudinal X-direction: secondary transverse beams are present only along the perimeter (see Figure 3). This spatial configuration of frames is widely spread in Italy also for buildings erected in seismic areas during the years 50 and 60. Hence, the structure lacks bi-directionality and has a *strong* X-direction, reflecting a typical configuration for RC buildings deemed to support mainly vertical loads, as it was in the case study analysed by Mulas &

Martinelli (2017), where the structural behaviour was dominated by the presence of strong and weak directions. A few load-bearing walls, located in the two cores could potentially contribute to a bidirectional bracing resisting system even though they show an unfavourable eccentric position.

The construction system of both buildings consists of precast elements (APE® precast system): single-storey reinforced vibrated concrete (RVC) column, self-supporting RVC beams and precast floors. Figure 5 shows a few details of the construction system. Additional cast in-situ concrete provides continuity at beam-to-column joints, even though such detail was not enforced, in non-seismic zones, by the Italian code on precast structures at time of design.

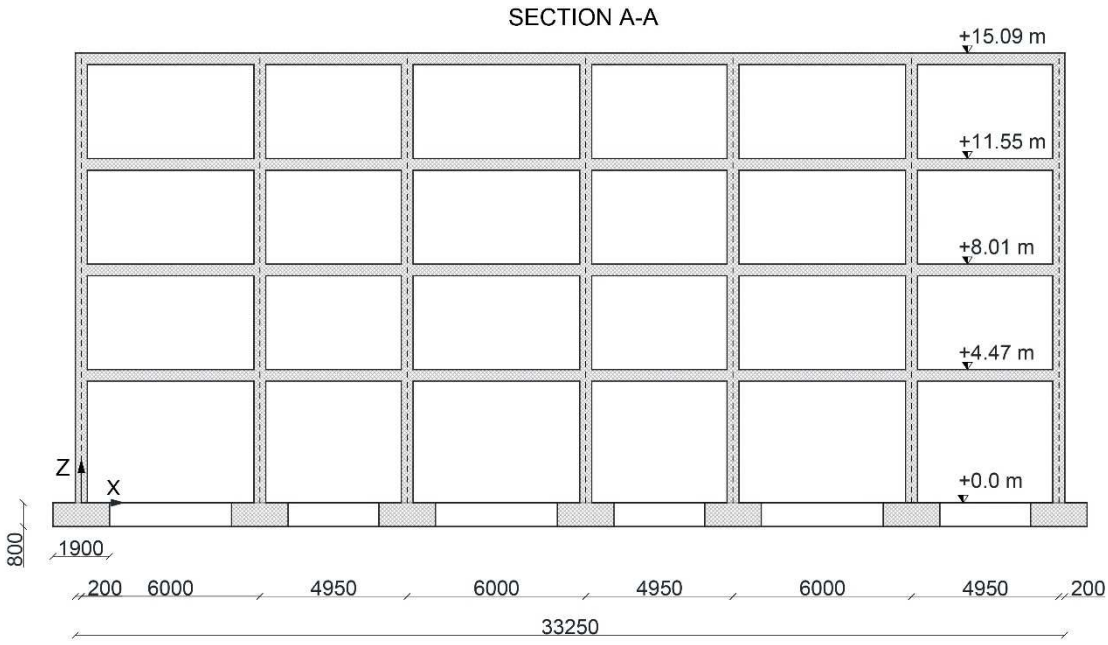

Figure 4 - Building B1: longitudinal section (units: mm).

Floors are made of precast RC one-dimensional slabs with steel trusses and polystyrene foam blocks forming the joists. Slabs are 240 cm wide and their whole thickness is equal to H = 40.5 cm (4.5+32+4 cm). The lower layer, 4.5 cm thick, ensures a REI 120 resistance against fire hazard, where the acronym REI identifies an element that must retain, for 120 minutes, the mechanical strength (R), the resistance to flames and hot gases (E), and the thermal insulation (I). A welded mesh with a diameter Ø6 and with spacing of 200 mm is placed in the cast in-situ top layer of concrete. Roof floors are flat, carrying an insulating layer, sheaths and gravel.

Columns are tapered, with sections reducing moving upwards, as shown in Table A1. All but three cross-sections are 40 cm deep; width is in the range 25-50 cm. Each column has lower protruding longitudinal bars and upper pockets: lower bars of each column fit into the pockets of the one below or of the foundation (Figure 5a). During construction, a column is plumbed and the pockets are sealed with a cast in-situ concrete. To ensure alignment and verticality of columns during erection (Figure 5b) a hole (either centred or eccentric) housing a tube is present

at the upper ends. Shear reinforcement is provided by Ø6 stirrups spaced of 20 cm, a detailing no longer allowed by both Italian and European codes. Perimeter infill walls, 40 cm thick, are made of 25 cm masonry blocks, 5 cm polyurethane layer and 10 cm RC precast outer panels, anchored outside the supporting columns.

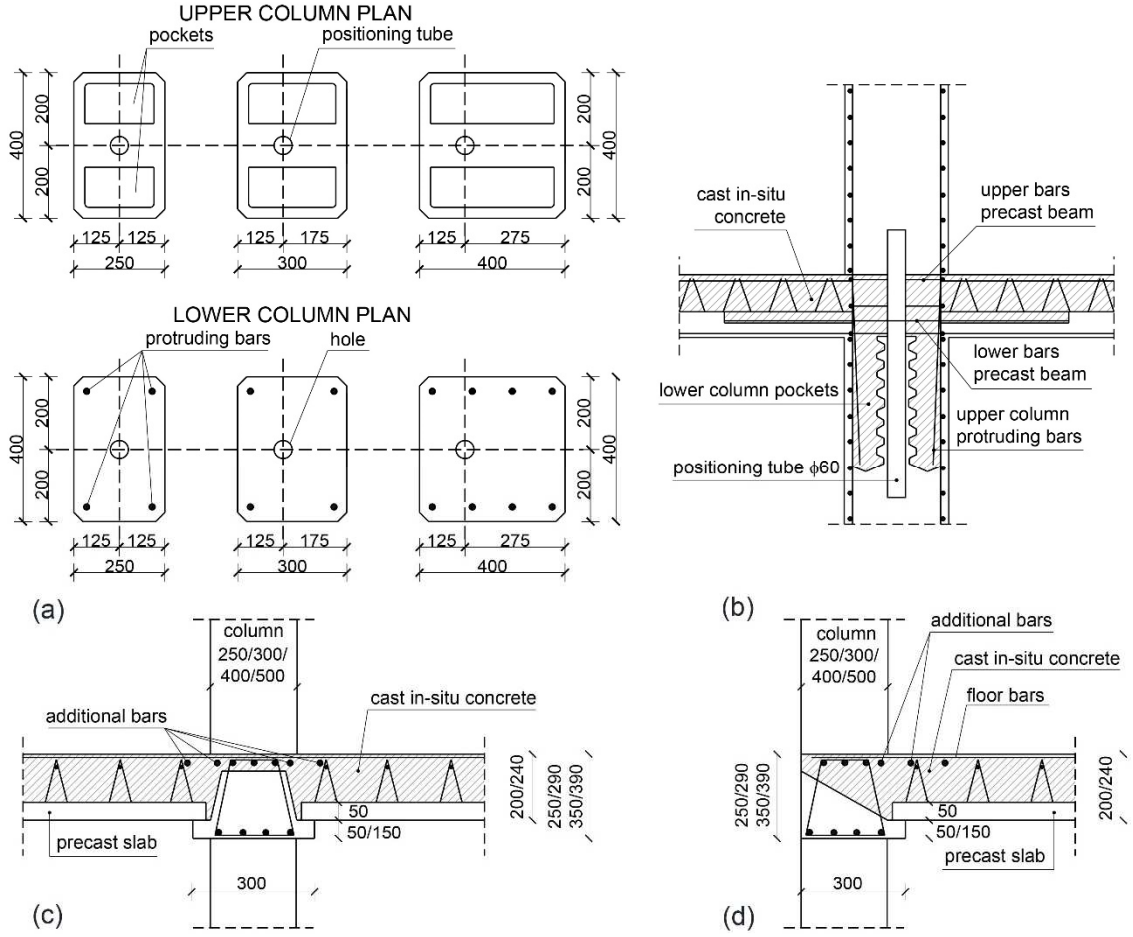

Figure 5 – APE® precast system, details for generic: a) columns cross-sections, b) beam-column joint, c) internal longitudinal beam and d) external longitudinal beam (units: mm).

All beams are 39 cm high. Transversal beams are rectangular, 30 cm wide. Longitudinal beams are of two types: the central ones, T-shaped, are 110 cm wide; the lateral ones, L-shaped, are 80 cm wide. The shape of non-rectangular cross-sections is due to the in-situ cast of the slabs extending up to the beams (Figure 5c-d). These elements lack in seismic detailing: in particular, stirrups spacing and geometry are constant along their length. Dimensions in Figure 5 are not exhaustive of the actual dimensions used in construction. The geometry of the joint reinforcement is not known.

The RC walls composing the lift core and the technical core were cast on site. They develop along the entire height of the building with a constant thickness of 20 cm. The lift core has an opening of 2.2 m at each floor, while the technical core has an opening only at the ground floor (Fig. 3). Only one of the available documents contains the construction detail of the reinforcement of a generic wall of the lift/technical core. In vertical, 2Ø12 spaced of 20 cm and 2Ø10 spaced of 20 cm are arranged for the first and last two floors, respectively. Horizontally, the

reinforcement is constant and equal to 2Ø8 spaced of 25 cm. Herein, this reinforcement is adopted for all the walls.-The document does not contain data on the details of connection of walls to adjacent beams.

Foundations are composed of RC footings 80 cm high, supported by piles and connected by RC beams 80 cm high and of different widths. There are seven types of footings, differing in size and in the number of piles on which they rest. The foundation system is only partially adequate, due to lack of connections in the two perpendicular directions between adjacent plinths.

FeB44k-class steel was used for all the structural elements, with a characteristic yielding strength f_{yk} = 430 MPa and an ultimate tensile strength f_{tk} = 540 MPa. Several types of concrete were used: a characteristic cubic strength (R_{ck}) of 25 MPa was used for foundations and walls; R_{ck} = 30 MPa was used for columns, infills, slabs, and R_{ck} = 45 MPa was used for beams. The lack of a complete knowledge of materials and geometry would require experimental activities to adopt the highest level of knowledge LC3 allowed by Italian Code for existing structures (equivalent to KL3 in EN 1998-3, 2005). Hence, in the following, the average knowledge level (LC2 or KL2) is assumed and material strengths are reduced by a confidence factor of 1.2, even though a very limited uncertainty affects the properties of the cast-in-factory concrete of beams and columns. The values of dead and live loads to be adopted in the structural analysis according to NTC 2018 (2018) are listed in Table 1.

Table 1 – Dead loads and live loads for each floor.

Floor (floor part)	Self-weight + furniture (kN/m^2)	Surface weight of partitions (kN/m^2)	Live loads (kN/m^2)
Fourth floor	6.5	-	1.5
First-second-third floor	7.0	7.05	5.0
Ground floor	7.0	7.05	5.0
Stairwell	6.5	-	4.0
Landings	6.0	-	4.0
Technical compartment	3.0	-	5.0

The plan of Building B2 is depicted in Figure 6. With a different but more favourable plan configuration, since cores have a reduced eccentricity, Building B2 adopts the same type of resisting system, structural elements and materials and the same values of load described for Building B1.

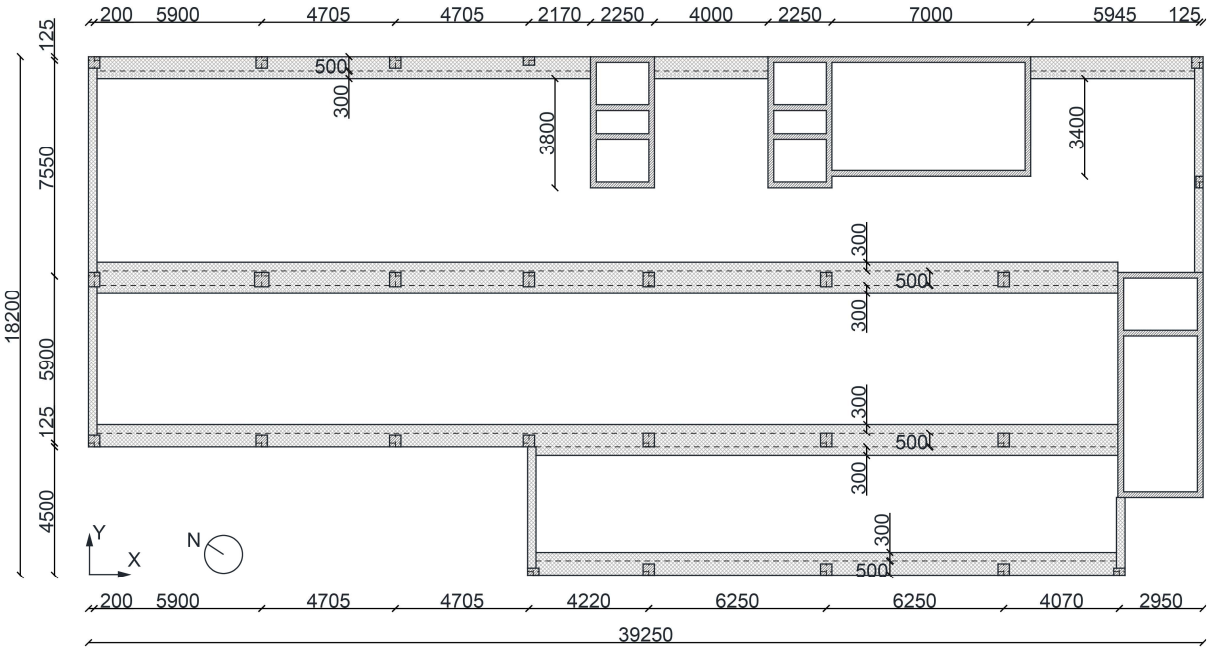

Figure 6 - Typical floor plan of Building B2 (dimensions in mm).

3 Structural Modelling

Structural models of the structures under study are developed by means of the SAP2000 (2018) finite element software, based on the original design documents and on the knowledge of the current state of the building. A linear model is built for static, modal and response spectrum analyses, while a nonlinear model is set for pushover analysis. In the latter, nonlinear behaviour is described through Mander's stress-strain model (Mander et al., 1988) for concrete, while a hardening elastic-plastic constitutive law with kinematic hysteresis is assumed for steel. Lumped plasticity elements are adopted by introducing automatic plastic hinges (SAP2000 2018) at the end sections of elements. The parameters necessary for the moment-plastic rotation angle relationships are taken from ASCE 41-07 (2007), Tables 10.7 and 10.8, depending on the value of internal forces, reinforcement ratios, material properties and sizes of beams, columns and walls. Tables 2 and 3 show the material properties for concrete and steel, respectively. As anticipated, strengths are reduced by the factor 1.2 corresponding to the knowledge level LC2.

Table 2 - Concrete properties. Note: E_c = Young modulus; f_{cd} = compressive design peak strength; ε_c = strain at the compressive peak strength; ε_{cu} = ultimate strain in compression

Material	E_c [MPa]	f_{cd} [MPa]	$\varepsilon_c \times 10^{-3}$	$\varepsilon_{cu} \times 10^{-3}$
C20/25	30076	17.0	2.0	3.5
C25/30	31311	20.4	2.0	3.5
C35/45	34462	30.5	2.0	3.5

Table 3 - Steel properties. Note: E_s = Young modulus; f_{yd} = yielding design strength; f_{td} = ultimate design strength; f_{yk} = yielding characteristic strength; f_{tk} = ultimate characteristic strength; ε_{sy} = yielding strain; ε_{su} = ultimate strain

Material		E_s [MPa]	f_{yd} [MPa]	f_{td} [MPa]	f_{yk} [MPa]	f_{tk} [MPa]	$\varepsilon_{sy}\times10^{-3}$	$\varepsilon_{su}\times10^{-3}$
FeB44k		200000	358	450	394	495	1.79	67.5

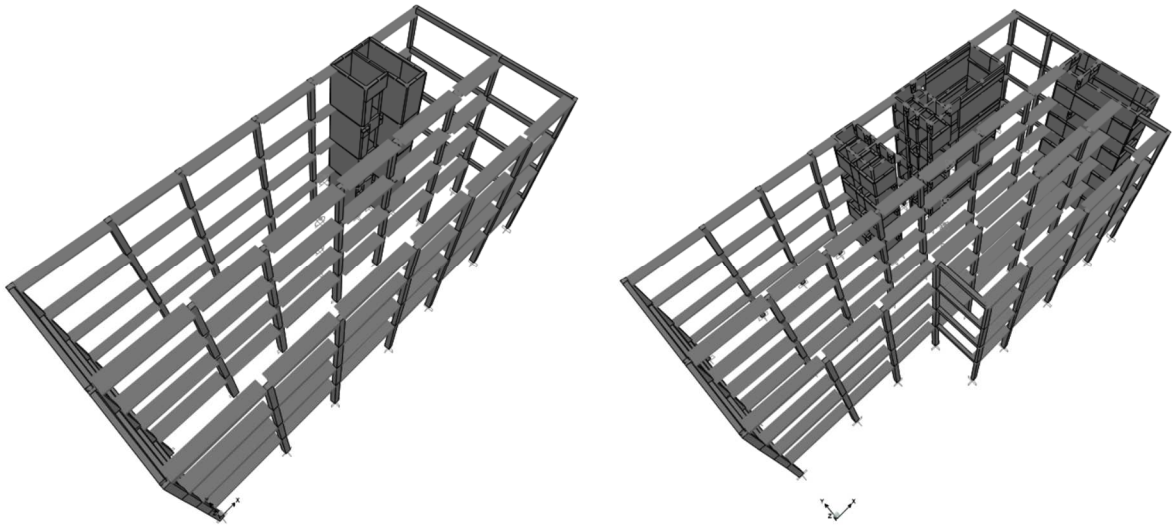

Figure 7 - FE model of Buildings B1 (left) and B2 (right).

Figure 7 shows the FE model of Buildings B1 and B2. Floors are modelled as rigid horizontal diaphragms, because of their very high in-plane stiffness. Beams and columns are modelled using two-node beam elements (6 DOFs per node), having a 3-D formulation including the effects of biaxial bending, torsion, axial deformation and biaxial constant shear deformation. A rigid zone length, equal to half of the beam-column joint length, is considered for both beams and columns. Columns are clamped at their base, accounting for the effect of a foundation system with high flexural stiffness.

Walls are modelled by using the "*wide beam*" formulation, i.e. using shear-deformable beam elements and introducing rigid links into the end nodes in order to consider the actual size of the section. Discretized connection between orthogonal walls is enforced by assuming vertical shear transmission at the floor levels. Connection to adjacent beams follows the geometric detail in Figures 3 and 6. At each floor, lintels centreline has the same vertical coordinate of the slab to comply with the rigid diaphragm hypothesis. A rigid zone length is adopted also for beam-wall connections, with a length equal to half of the actual length of the connection. Infills walls, lacking the proper details of the connection to the columns, are not considered in the FE model. Mass of resisting elements (beams, columns, walls) is automatically accounted for, while masses of slabs, infills, landings and stairs are assigned, for each floor, to a master node, located at the centre of mass of the floor. The moment of inertia about the vertical axis is also accounted for. Since during a seismic event RC structural elements undergo cracking, 30% and 20% stiffness reduction in terms of area and moment of inertia are considered for Life Safety Limit State

(LSLS; no-collapse requirement in EC8) analysis and Damage Limit State (DLS) analysis, respectively. The stiffness reduction applied to columns is justified in the light of the results, shown in Section 4.1, in terms of both capacity and ductility. Tables 4 and 5 show the results of the modal analysis performed for B1 and B2, respectively, assuming the 30% stiffness reduction. Coupled torsional/transversal modes appear in both cases.

Table 4 - *Modal properties of B1 assuming a 30% stiffness reduction due to cracking.*

Mode	Period [s]	Modal Participating Mass [%]			Cumulative Modal Participating Mass [%]			Mode type
		M_X	M_Y	M_{RZ}	M_X	M_Y	M_{RZ}	-
1	1.290	7.9	36.3	42.1	7.9	36.3	42.1	Torsional/Transversal
2	0.556	74.9	9.1	0.4	82.8	45.4	42.5	Longitudinal
3	0.420	0.1	2.5	9.5	82.8	47.9	52.0	Torsional
4	0.310	4.1	38.5	38.2	86.9	86.4	90.2	Transversal/Torsional
5	0.233	0.4	1.0	1.3	87.3	87.4	91.5	Torsional/Transversal
6	0.173	10.9	2.5	0.0	98.2	89.9	91.5	Longitudinal/Transversal

Table 5 - *Modal properties of B2 assuming a 30% stiffness reduction due to cracking.*

Mode	Period [s]	Modal Participating Mass [%]			Cumulative Modal Participating Mass [%]			Mode type
		M_X	M_Y	M_{RZ}	M_X	M_Y	M_{RZ}	-
1	0.525	7.2	47.5	33.2	7.2	47.5	33.2	Transversal/Torsional
2	0.252	59.3	21.0	3.1	66.5	68.5	36.3	Longitudinal/Transversal
3	0.186	13.6	14.3	53.7	80.2	82.8	90.0	Torsional/Transversal
4	0.169	3.2	10.0	0.6	83.4	92.9	90.7	Transversal
5	0.095	0.1	0.7	0.6	83.5	93.6	91.2	Transversal
6	0.079	10.8	3.1	0.5	94.3	96.6	91.7	Longitudinal/Transversal

As already stated, Building B1 is not regular in plan, due to lack of symmetry caused by the eccentricity of the two cores. In addition, it belongs to the class of torsionally deformable buildings (as defined by both Italian and European Codes), also due to the unidirectional texture of the beams. The fundamental period is associated with a torsional modal shape. Building B2 is also torsionally deformable, but, owing to the reduced eccentricity of lift cores, is characterized by shorter periods and the torsional mode appears as 3rd mode only. For both buildings, small columns' cross-sections contribute to the 1st mode period elongation.

4 Assessment of Seismic Vulnerability

The seismic action on Building B1 is represented by a response spectrum depending on the site seismic hazard and on the soil type, in accordance with the Italian Building Code (NTC 2018, 2018) and coherent with the general

concepts of EC8. The status of strategic importance of the building is associated with a nominal life $V_N = 100$ years associated to a coefficient of usage $C_u = 2$, resulting in a reference period $V_R = C_u \times V_N = 200$ years. Hence, large return periods are associated with the LSLS and DLS, equal to 1898 years ($P_{VR} = 10\%$ in Figure 1) and 120 years ($P_{VR} = 81\%$), respectively. The soil type is of class D, the topographic amplification factor is 1.0. The resulting horizontal peak ground acceleration (PGA) is 0.258*g* for the LSLS and 0.097*g* for the DLS. The corresponding elastic and design response spectra are depicted in Figure 8, where vertical lines indicate the periods of the first three modes of Building B1 (Table 4). The very long first mode period falls in the spectrum descending part, i.e. the constant velocity branch. The assessment adopts the full spectrum, as for a new structure. However, the LSLS design spectrum is obtained from the elastic one by adopting a behaviour factor $q = 1.5$, smaller than the value one would adopt in design. In fact, due to the torsional deformability of the structure, the q factor cannot be larger than 2; a further reduction is adopted due to the lack of adequate detailing to guarantee a sufficient ductility level. These assumptions will be revised in the retrofitting phase.

Following prescriptions of NTC 2018 (2018), the analyses do not account for vertical excitation and for spatial variability of the motion. The former can be neglected because there are no prestressed, suspended, cantilever or longer than 20 m elements, even though the ground acceleration $a_g > 0.15g$. The latter was not considered due to the limited plan dimension of the building and to the presence in the longitudinal direction of beams connecting footings.

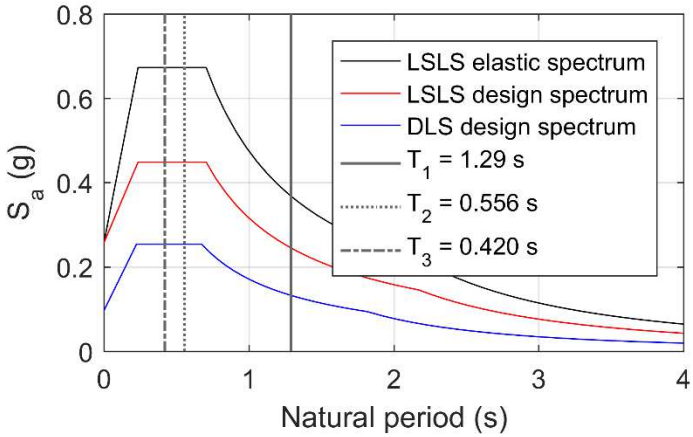

Figure 8 – Elastic and design spectra, 5% damping. T_1, T_2 and T_3 = first three periods of Building B1.

4.1 Response spectrum analysis

The response spectrum analysis (RSA) is only performed for the horizontal components of seismic motion. Accidental eccentricities of centres of mass are introduced to account for the uncertainties about the position of these points and the spatial variability of seismic motion. A total of 32 load combinations arises when the four

possible positions of the centre of mass are associated to the 8 possible combinations of the seismic action components in both horizontal directions. Seismic effects are determined by applying the 30% combination rule. Dead and live loads are considered according to the seismic combination defined in both NTC 2018 (2018) and EN 1990 (2005). Inertial masses acting during the earthquake are defined according to the Italian Code.

All the elements are checked with regard to the LSLS design spectrum: beams are verified in bending (M) and shear (V), columns in combined moment and axial force (N) and in shear. Walls are verified in shear, axial force and bending. The rate of action ξ_E carried by the i-th element is defined in bending, in bending coupled with axial load and in shear, as the ratio between capacity (M_{Rd}, $M_{Rd}(N)$, V_{Rd} respectively) and demand (M_{Ed}, $M_{Ed}(N)$, V_{Ed} respectively) as it follows:

$$\xi_E^M = \frac{M_{Rd}}{M_{Ed}} \tag{1}$$

$$\xi_E^{M(N)} = \frac{M_{Rd}(N)}{M_{Ed}(N)} \tag{2}$$

$$\xi_E^V = \frac{V_{Rd}}{V_{Ed}} \tag{3}$$

The non dimensional parameters ξ_E^M, $\xi_E^{M(N)}$, ξ_E^V are computed for all the structural elements. Values smaller than unity denote an insufficient capacity. Figures 9, 10 and 11 show the results for beams, columns and walls, respectively. For the sake of compactness, in these figures values larger than one were set equal to unity. A black circle, a blue square, a red triangle and a green rhombus indicate results at 1st, 2nd, 3rd and 4th floor, respectively.

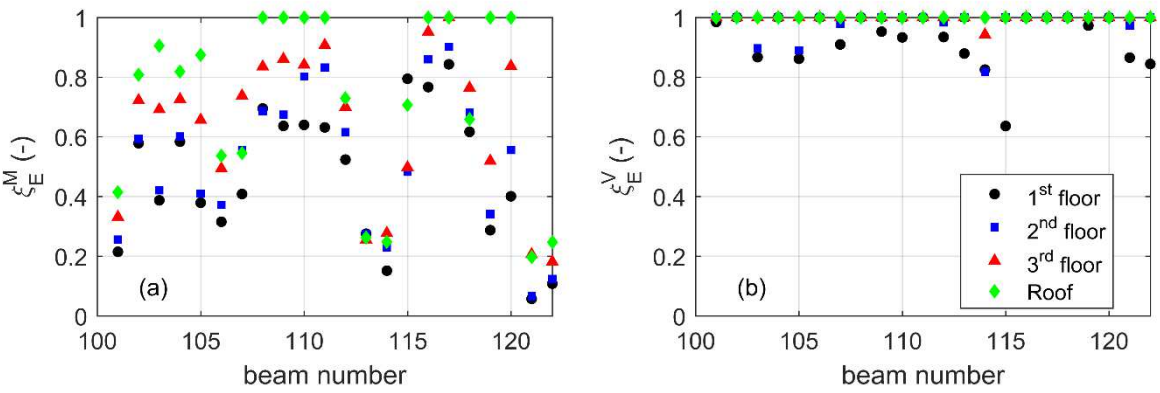

Figure 9 - Beams assessment: a) bending, b) shear.

For beams, numbered from 101 to 122 (see Figure 3), all critical cross-sections are analysed (both ends and mid-span) and the worst result for each beam is represented in Figure 9. For columns, biaxial bending and axial force are considered, taking into account both positive and negative sign of the spectral value of the latter. Figure 10a shows the most critical situation for each column.

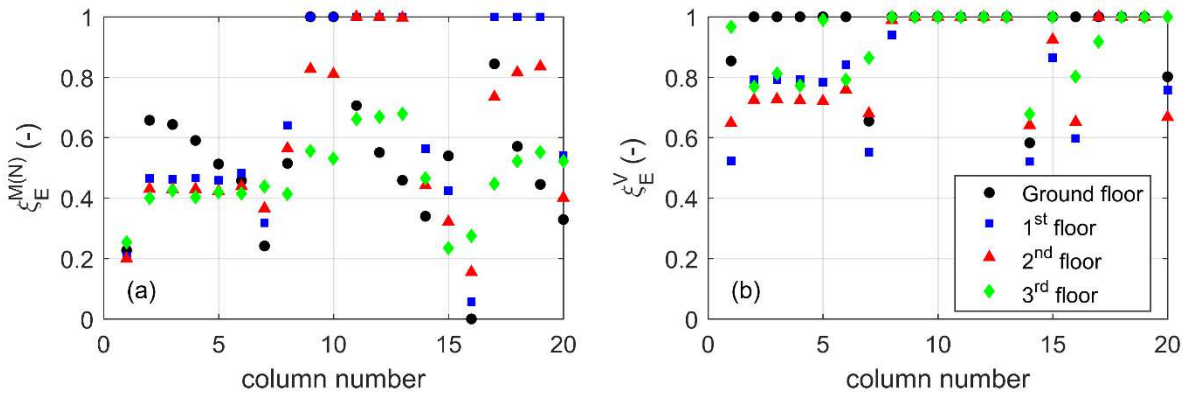

Figure 10 - Columns assessment: a) bending and axial force, b) shear.

Frame elements show deficiencies in bending and shear. Only 9 out of 88 beams comply with flexure requirements and, in some cases, strength covers only 10% of demand. The situation is better for shear requirements, satisfied by 68 elements, with strength covering at least 60% of demand. For columns, only 12 out of 80 meet compression and bending requirements, but 42 verify shear resistance. The result worsens moving upwards, due to the loss of the favourable contribution of axial force. An opposite trend is observed for beams. Column C16, at the left of the elevator core, is subjected to a tension larger than the strength offered by longitudinal reinforcement.

Walls are the most critical elements. Due to their stiffness, they attract a significant rate of seismic action but their reinforcement ratio is not sufficient to provide the corresponding strength. Due to the low value of axial force due to gravity loads, only 3 out of 29 wall elements are verified in tension and bending and 22 are subjected to a tension exceeding the strength of longitudinal reinforcement (results are not shown here for the sake of brevity). Figure 11 shows that no wall is verified in shear, showing in some cases percentages around 5%.

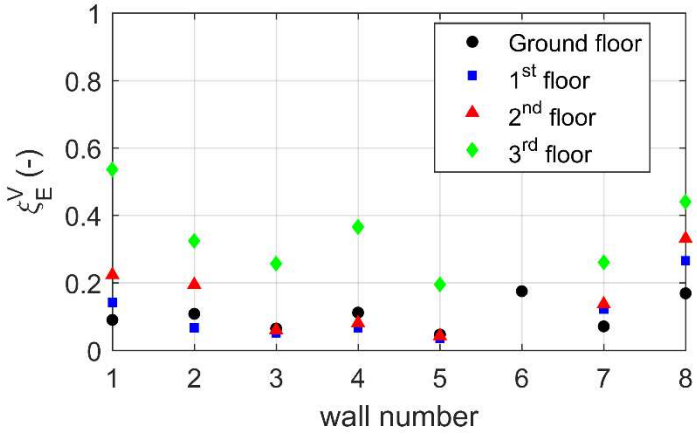

Figure 11 - Walls assessment: shear (see Figure 3 for wall numbering).

The Italian seismic code also poses a few requirements for deformability and ductility. For the first aspect, a minimum distance between two adjacent buildings is required to prevent pounding phenomena. For the case under study, a realizable value of gap equal to 7.8 cm should be present at top floor. The sum at top floor of LSLS

horizontal spectral displacements for Buildings B2 and B1 is equal to 11.6 cm, exceeding the minimum value required by the Italian code. The larger contribution, 9.3 cm, is due to B1.

Inter-story drifts under DLS seismic action are computed for Building B1, to avoid non-structural damage that would make the construction temporarily unfit for use. The code requirement is satisfied at each floor along the longitudinal X-direction (Figure 3), but only at the top floor along the transversal direction, that confirms it to be the weak direction for Building B1.

For the second aspect, the available ductility in curvature is computed for all structural elements. All beams respect ductility prescriptions, while columns and walls are very far from fullfilling ductility requirements. Only 5 out of 60 nodes respect the *"strong column - weak beam"* criterion. The results worsen moving upwards since beams dimensions are constant while columns are tapered, with a reduction of reinforcement area. Hence, brittle collapse mechanisms where beams do not develop their full capacity, as soft/weak story, could occur. Since no strategy about the ductile properties of elements was taken into account in design, these results confirm the soundness of the choice of a q-factor equal to 1.5 for the original structure.

4.2 Pushover analysis

Response spectrum analysis highlights the deficiencies of the individual structural elements (columns, beams, walls). The nonlinear static analysis, or pushover analysis, is adopted to investigate how these deficiencies influence the overall behaviour of the structure and to analyse the collapse mechanisms. In this analysis, gravity loads acting in the seismic combination are applied first. Subsequently, an incremental pattern of horizontal forces is applied, monotonically increasing up to the collapse limit state. Neglecting the accidental eccentricity accounted for in RSA, at each floor forces are applied at the centre of mass (the master node), that is in eccentric position with respect to the centroid of the rectangular plan area. Forces are distributed along the height according to an estimate of the pattern of floor inertia forces, considering two force distributions as prescribed by both Italian and European Code, one from Group 1 of the main distributions, the other from Group 2 of secondary distributions. The former, denoted as “type 1”, is proportional to the inertia force at each floor calculated through a multimodal linear dynamic analysis. The latter, denoted as “type 2”, corresponds to a uniform force distribution along the height of the construction.

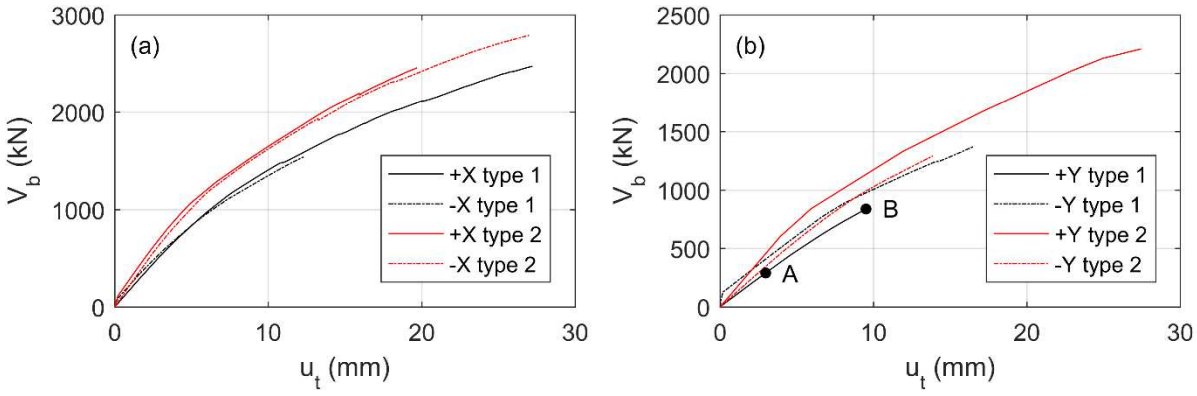

Figure 12 – Capacity curves for seismic forces applied: (a) in X-direction; (b) in Y-direction.

As allowed by the Italian Code NTC 2018 (2018) for nonlinear static analysis, each of the two horizontal components (X- and Y-direction, see Figure 3) is applied separately. The model is subjected to a nonlinear, monotonic, pushover analysis, adopting the centre of mass of the last floor as control node. The analyses are in displacement control, with a displacement step of 0.25 mm, a maximum number of iterations per step equal to 40, and a tolerance of 0.001 mm on the displacement. Equilibrium at each load step is imposed with the Newton–Raphson method. The resulting capacity curves in terms of top displacement (u_t) versus base shear (V_b) are shown in Figure 12a and 12b, for both type 1 and type 2 distributions and forces acting in ±X and ±Y directions, respectively.

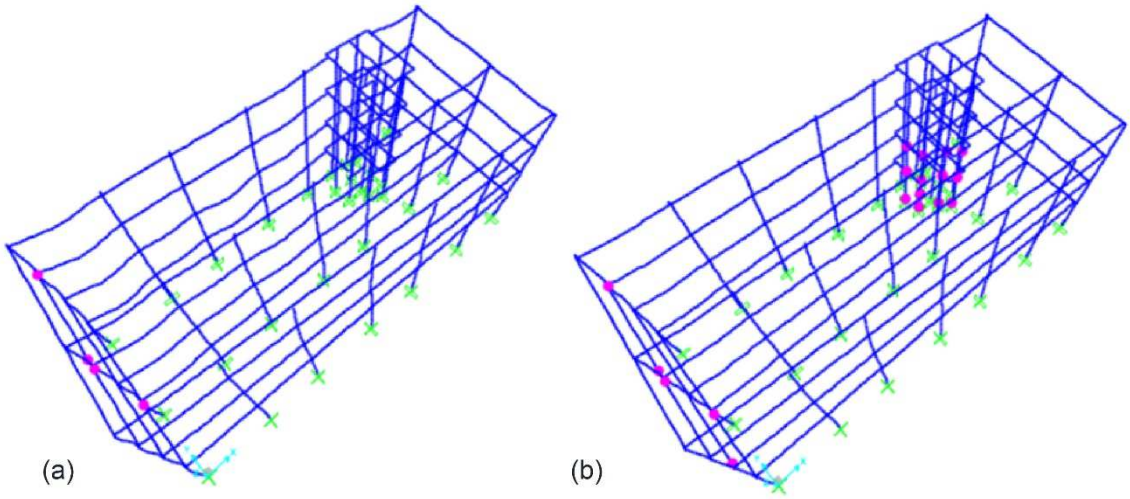

Figure 13 – Plastic hinges evolution for seismic load forces of type 1 applied along +Y direction: (a) load step 12 (point A in Fig. 12b) and (b) load step 37 (point B in Fig. 12b).

In Figure 12, the most critical load condition is given by seismic load in the positive Y-direction with a force distribution of type 1. In this case the structure can sustain only a very small top displacement equal to 9.5 mm. In the X-direction, the structure has a larger, although limited, displacement capacity equal to 12.3 mm. In the Y-direction a lack of both ductility and strength is detected, confirming that the weak direction of the building is the transverse direction (see the value of the base shear in Figure 12b). For the most critical load condition, a brittle

failure was observed in the walls due to the level of tensile forces, exceeding the capacity provided by the limited amount of steel reinforcement and preventing the full development of frames capacity.

Figure 13 shows the evolution (i.e., the formation and development) of plastic hinges, for the most demanding seismic load combination (+Y direction, type 1 distribution) at two different load steps. In particular, Figure 13a refers to the load step 12 (point A in Fig. 12b), while Figure 13b shows the plastic hinges development at the end of the analysis (load step 37, point B in Fig. 12b). The evolution of plastic hinges confirms that walls are the weakest structural elements under seismic actions. The wall base cross-sections plasticize prematurely at low values of the horizontal seismic forces, due to the combined effect of axial force and bending moment. Plastic hinges develop first on the columns and then on the beams, confirming the non-fulfilment of the hierarchy strength principle of "*weak beam-strong column*".

5 Retrofitting Strategies

The seismic analyses pointed out the drawbacks to be limited. At a global/structural level, a desirable retrofitting intervention should modify the building response, eliminating the torsional deformability associated with a long, first mode period, while limiting the risk of pounding on the adjacent building connected with the excessive deformability. At the element level, it is necessary to provide strength and ductility. Retrofitting strategies aiming to reduce the structural role of either the walls or the frames, transforming them in secondary elements (NTC 2018, 2018; EN 1998-1, 2005), are not applicable to this case. On one side, the good quality of the framed precast structure, in terms of construction system (continuity at nodes) and material properties, suggests maintaining their role as a lateral force resisting system. On the other side, the weakness of the walls indicate that they are not strong enough to be the primary elements. Base isolation appears practically unrealizable due to the lack of a basement. Moreover, it could be impossible to accommodate the large relative displacements between adjacent buildings involved in this technique.

In this work, two retrofitting strategies are devised that respect the constraint, dictated by the building usage, of inserting new elements in the perimeter only. They act in the same way at the element level, where the strengthening of the existing frames is pursued through the addition of an external steel reinforcement with the CAM® (Active Confinement of Masonry) system (Marnetto et al., 2018; Monti et al., 2016). At a global level, the aim of regularizing the torsional mode and relieving the overstress of existing walls is reached by acting in two opposite ways on the building stiffness, either increasing or decreasing it.

The design philosophy of the proposed interventions follows the prescriptions of the NTC 2018 (2018) for existing buildings that lists two main categories of retrofitting interventions, depending on the value of the ratio ζ_E between

the maximum seismic action that the structure can withstand safely and the seismic action that would be used for a new building. A value of $\zeta_E = 1$ characterizes the *conformation* intervent, when the existing building is made adequate to sustain the whole seismic input. For $\zeta_E < 1$ an *improvement* intervention takes place. In both cases, the value of the other actions acting simultaneously is the same as for new buildings (NTC 2018, §8.3). For the case study, given the lack of capacity of the original structural system and the status of strategic building, a value of $\zeta_E = 0.6$ is assumed as a realistic limit to be pursued. This represents the minimum value that must be reached in any retrofitting intervention on a strategic existing building (§8.4.2).

5.1 Stiffening strategy

The stiffening strategy, schematically shown in Figure 14, aims to increase the structural seismic capacity. In the stiffening intervention, a new transverse RC shear wall is inserted in the structural system, in a position where a foundation beam is present. The new vertical element, extending along the whole building height, is introduced along the plan perimeter between the columns C7 and C14, replacing the external infill between the two. This choice allows use of internal spaces during refurbishment works. The new wall is intended to reduce the demand on existing walls. Its position is capable of regularizing the torsional mode shapes and stiffening the structural system, inserting a resisting element along the building's weak direction. The wall is designed with a concrete class C35/45 and reinforcement bars of type B450C. The wall thickness is 40 cm and its width is constant in elevation. Its connections to the existing elements are carefully detailed.

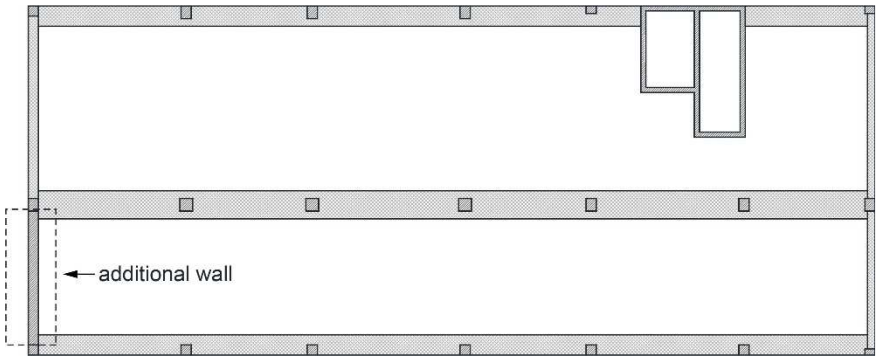

Figure 14 – Stiffening strategy for Building B1: addition of a new RC wall.

To assess the effect of this strategy on the global behaviour, a modal analysis is performed in the post-intervention state, assuming again a 30% reduction of stiffness to account for cracking. The results in Table 6 show that the natural periods undergo a reduction with respect to the initial state (Table 4) up to 56%, 42% and 43% for the first three modes respectively, as it can be appreciated in Figure 15. Coupling of modes vanishes, the torsional mode shifts to the third position, the value of the first mode period is very close to that of Building B2 in Table 5. These findings highlight the effect of the reduction of the eccentricity between the centre of stiffness and that of mass,

confirming the regularization of the torsional mode. Moreover, with the wall insertion in the transverse direction, the longitudinal one becomes the weakest direction.

Table 6 - *Modal analysis of retrofitted Building B1, stiffening strategy.*

Mode	Period [s]	Modal Participating Mass [%]			Cumulative Modal Participating Mass [%]			Mode type
		M_X	M_Y	M_{RZ}	M_X	M_Y	M_{RZ}	-
1	0.563	82.9	0.6	1.2	82.9	0.6	1.2	Longitudinal
2	0.325	1.6	70.6	8.8	84.5	71.2	10.0	Transversal
3	0.238	1.4	7.9	67.0	85.9	79.1	77.0	Torsional
4	0.178	12.0	0.1	1.9	97.9	79.2	78.8	Longitudinal
5	0.097	1.8	0.4	0.1	99.7	79.5	78.9	Longitudinal
6	0.092	0.0	13.7	2.4	99.7	93.2	81.3	Transversal
7	0.069	0.3	0.0	0.0	99.9	93.2	81.3	Longitudinal
8	0.060	0.0	4.2	16.2	100.0	97.5	97.6	Torsional

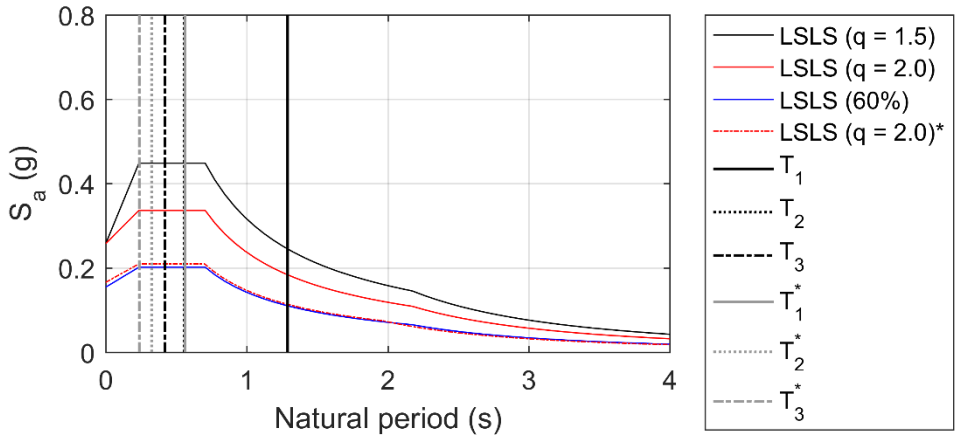

Figure 15 - Design spectra at LSLS before and after retrofitting. T_1, T_2, T_3 and T_1^*, T_2^*, T_3^* = first three periods of Building B1 before and after stiffening retrofitting.

An accurate design of the additional wall leads to an increase in the available ductility and overall strength which, together with the change in structural type due to the regularization of the torsional mode, allows for the adoption of a *q*-factor = 2, corresponding to a mixed system equivalent to uncoupled walls, as defined by NTC 2018 (2018) and EN 1998-1 (2005). Moreover, the factor ζ_E = 0.6 is applied to the initial seismic input, scaling in the same way the whole response spectrum. Figure 15 shows the comparison between the LSLS spectra scaled for the two *q*-factors considered, and the LSLS spectrum with $q = 2$ further scaled to 60%. To appreciate the effect of this reduction, the same figure shows that the design spectrum corresponding to the reference period V_R=50 years of the ordinary buildings (labelled as *LSLS (q = 2.0)**) practically coincides with the reduced spectrum. In this way, even though not explicitly stated in the Italian Code, the earthquake performance of the building is shifted from

the Safety Critical Objective to the Basic Objective (Figure 1). Finally, the shift of the first mode period, leading to an increase of demand, is well visible.

Table 7 – *Total base shear and frames percentage, original configuration vs. stiffening strategy.*

Direction	Base shear before retrofitting [kN] *q=1.5*	Frames %	Base shear after retrofitting [kN] *q=2*	Frames %	Base shear after retrofitting [kN] *q=2, LSLS 60%*
X	10474	22	7048	17	4229
Y	9717	21	7921	2	4753

A response spectrum analysis is carried out on the post-intervention building. Table 7 shows the results in terms of base shear force in the X- and Y-direction. The 2nd and 3rd columns list, for the original configuration, the base shear and the percentage carried by the frames, respectively. The 4th and 5th list the same values, for the post-intervention configuration, while the 6th column accounts for the reduction in the design spectrum. The demand in terms of seismic actions on the retrofitted structure is reduced by 60% along the X-direction and by 52% along the Y-direction, respectively. The percentage of demand on frames reduces in X-direction and goes almost to zero in the transverse Y-direction, where the new wall is added. In this configuration, beams and columns have the capacity corresponding to the demand posed by the reduced design spectra, hence reaching what is defined "*seismic improvement*" by the Italian Code (NTC 2018, 2018), with the exception of few frame elements, having the required shear capacity but not the bending capacity. For these elements, a strengthening through additional longitudinal bars welded at the end sections to angular profiles allows to balance the demand of the LSLS spectrum scaled to 60%. The horizontal displacement at LSLS, at the interface with the adjacent building, is now equal to 6.5 cm, a value compatible with the current construction practices and sufficient to avoid the pounding phenomenon. The DLS deformability checks are now satisfied in both directions due to the addition of a very stiff element along the original critical direction (see Section 4). However, a few critical elements within the core still reveal deficiencies, under both eccentric axial tension and shear. At ground floor, the transverse wall W3, and the longitudinal W1 and W5 walls (Fig. 3) have a ξ_E index in the range 0.4-0.55. The wall W5, that provides continuity between the two beams B113 and B114 in the North frame (see Figure 3), is in the same range also at first and second floor. A strengthening through the CAM® system does not suffice to raise the ξ_E index to the unity for these walls.

5.2 Softening strategy

The second strategy aims to weaken the building, reducing its stiffness and thus the seismic demand. In the softening intervention, the existing RC walls are replaced by a frame system of columns 40×50 cm and beams in transverse (30×39 cm) and longitudinal directions (80×39 cm), as shown in Figure 16. To eliminate the torsional deformability, the cross-sections of columns C7 and C14 are increased to 40×70 cm. The new elements are designed with a concrete of class C35/45 and reinforcement bars B450C. A modal analysis is performed to assess the effect of the intervention on the global structural behaviour.

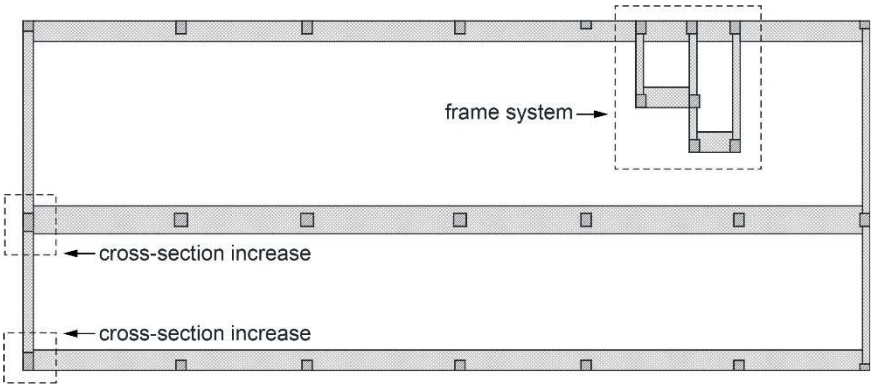

Figure 16 – *Softening strategy for Building B1.*

Table 8 - *Modal analysis of retrofitted Building B1, softening strategy.*

Mode	Period [s]	Modal Participating Mass [%]			Cumulative Modal Participating Mass [%]			Mode type
		M_X	M_Y	M_{RZ}	M_X	M_Y	M_{RZ}	-
1	1.648	0.0	75.3	5.7	0.0	75.3	5.7	Transversal
2	1.195	6.4	6.4	73.1	6.4	81.6	78.8	Torsional
3	1.026	84.0	0.5	5.9	90.4	82.1	84.7	Longitudinal
4	0.466	0.0	12.9	0.7	90.4	95.1	85.4	Transversal
5	0.372	1.4	0.2	9.4	91.8	95.2	94.8	Torsional
6	0.339	6.7	0.0	1.4	98.5	95.3	96.2	Longitudinal

The results of the modal analysis in Table 8, for modes having a participating mass larger than 5%, show a significant period elongation, due to the change in structural type from a mixed system to a frame system, with T_1 going from 1.290 to 1.648 s, with a 27% increase. The first mode is a translation in Y-direction. The torsional mode shifts to the 2nd position, highlighting the reduction of the eccentricity between centres of stiffness and mass and the regularization of the torsional mode. This fact and the change of structural typology allow to consider a behaviour factor higher than that adopted in the analyses on the original building. However, due to the lack of

ductility of the original frame, a *q*-factor equal to 2 is chosen also in this case. A LSLS analysis considering only 60% of the seismic input (see Figure 15) is carried out on the post-intervention situation. Base shear on the retrofitted structure is significantly lower than in the original structure, undergoing a reduction by 69% along X direction and by 75% along Y direction, respectively (Table 9). However, in this case about 70% of the base shear in both directions must be balanced by the original frames and it turns out that beams and columns have the required capacity in shear but not in bending. For beams, an additional reinforcement, designed using the CAM® system, suffices to provide the required bending capacity to all the elements, but the beam included between C7 and C14 at first, second and third floor. Hence, the stiffening of these columns implies an increase of internal forces also for the beams connecting them. For columns, only 55 out of 80 elements reach the required capacity. Strengthening is not possible in cases where the amount of necessary reinforcement would not satisfy the NTC 2018 limit (§7.4.6.2.1) on the maximum ratio between reinforcement and concrete areas. The required amount would result in a brittle beam behavior that, in turn, would not correspond to the adopted *q*-factor. In the softened configuration, the structure is more deformable. The horizontal displacement at LSLS at the B1-B2 interface is equal to 15 cm, even larger than in the original configuration and the DLS deformability checks are not satisfied along either of the two directions.

Table 9 – *Total base shear and frames percentage, original configuration vs. softening strategy.*

Direction	Base shear before retrofitting [kN] *q=1.5*	Frames %	Base shear after retrofitting [kN] *q=2*	Frames %	Base shear after retrofitting [kN] *q=2, LSLS 60%*
X	10474	22	5643	72	3278
Y	9717	21	4001	68	2401

5.3 Increase of seismic capacity due to the retrofitting strategies

The benefits/limitations of the two retrofitting methodologies investigated in this study are compared with the performance of the original un-retrofitted building in terms of strength of each structural members (i.e., beams, columns and walls), accounting for the reduction in the design spectrum (q = 2, *LSLS*, ζ_E = 0.6).

The rate of action ξ_E defined in Eqs. (1-3), for bending (ξ_E^M), for bending coupled with axial load ($\xi_E^{M(N)}$) and for shear (ξ_E^V), respectively, is herein evaluated for the results of RSA on the original building and after the application of the two retrofitting interventions. For the sake of brevity, only the ground floor columns, ground floor walls and first floor beams are examined in the following. Figure 17 compares the rate of action ξ_E^M in beams at the first floor. The benefits of the strengthening intervention (labelled as “ret. #1” in Figure 17) over the original and

softening solution are clearly visible, while only limited improvements on the original building are achieved with the softening intervention (labelled as "ret. #2" in Figure 17).

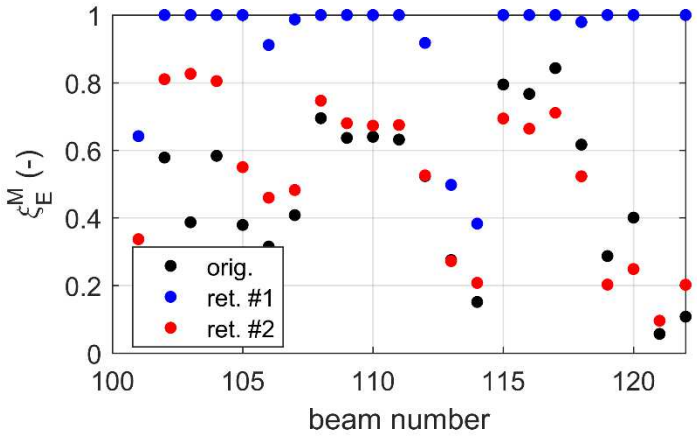

Figure 17 – Rate of action factors in beams at the first floor under bending moment action: comparison of original building ("orig.") with the two retrofitting strategies ("ret. #1" and "ret. #2")

Figure 18 presents the rate of action $\xi_E^{M(N)}$ in columns at the ground floor. The stiffening intervention guarantees a safe conditions for almost all columns. Beneficial effects can be appreciated also with the application of the softening intervention although many columns still need a local intervention.

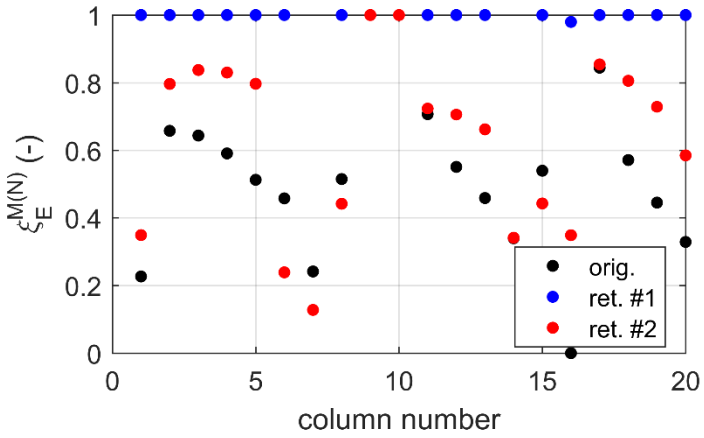

Figure 18 – Rate of action factors in columns at the ground floor under bending and axial force: comparison of original building ("orig.") with the two retrofitting strategies ("ret. #1" and "ret. #2")

Finally, Figure 19 compares the rate of action ξ_E^V in walls at the ground floor. Higher values are obtained after the application of the stiffening intervention compared to the original un-retrofitted building, although ξ_E^V in walls remains well below the unit.

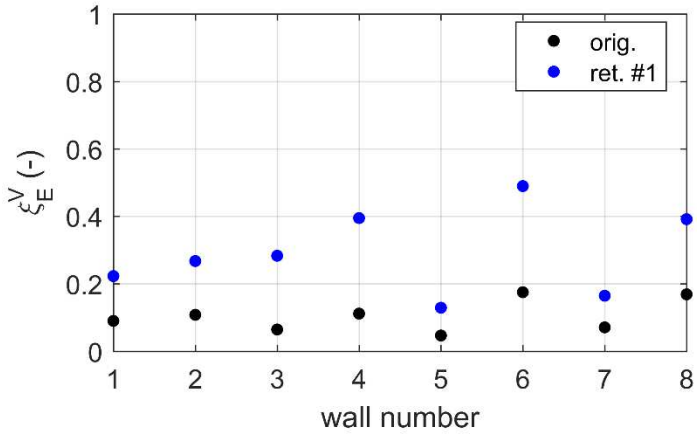

Figure 19 – Rate of action factors in walls at the ground floor under shear force: comparison of original building ("orig.") with the stiffening strategy ("ret. #1").

Numerical results obtained from RSA show that the regularization of the torsional mode, accomplished by both strategies, does not suffice to eliminate the structural deficiencies of the building. However, the lack of capacity in the retrofitted configuration of the stiffening strategy is such that local interventions with the CAM® System suffice to fill the gap with the demand corresponding to the reduced seismic input. The only notable exceptions remain, as already stated, in some wall of the cores.

6 Discussion of results

The seismic behaviour of the building at study is well characterized by the analyses performed in the vulnerability assessment and in the post intervention state for two different retrofitting strategies. In the original state, frames provide approximately the same fraction of base shear in the two directions. This fact can be explained with the cross-section geometry, since in the central frame at ground floor several sections have a width greater than the depth. Core walls attract about 80% of the base shear, since, differently from columns, they have a constant stiffness along the height. The building geometry, with unidirectional frames and eccentric cores, is the origin of the occurrence of coupled torsional/transversal modes. In this case study, the main effect of the lack of bi-directionality of frames is not the significant presence of a strong and weak direction (as it was in Mulas & Martinelli 2017) but the amplification of the role of the torsional mode, arising from the eccentricity of the cores. The vulnerability assessment is based on response spectrum and pushover analyses. The former adopts the full spectrum of a strategic building and a q-factor equal to 1.5, whose choice appears correct when ductility checks are performed. The latter shows that the low reinforcement ratio of walls can limit the full development of the frames capacity.

Retrofitting is pursued at both global and local level. At global level, the regularization of torsional modes is reached with two different strategies, either stiffening or softening the building. In the first case, an additional

wall is added in the transverse direction; in the second, core walls are substituted by a new frame system. Even though both strategies are successful in eliminating torsional deformability and coupling between transverse and torsional modes, the first one is to be preferred to the second on the ground of retrofitting at local level, where the same technique, based on the adoption of the CAM system, is used. In fact, in the stiffening strategy, where the frames' contribution is exploited to its best in the plane of the frames, a successful retrofitting is reached for them. This is not accomplished in the second strategy that eliminates the cores contribution and loads the frames beyond their capacity. Moreover, in the softening strategy, the frame deformability increases to an unacceptable level, that alone would be sufficient to discard it.

Two points need to be underlined. First, the adoption of a different q-factor in the assessment and retrofitting phase, where the lower q-factor corresponds to the building situation with respect to current code, while the higher is coherent with the advantages brought by the retrofitting intervention. Secondly, the reduced spectrum adopted in the retrofitting phase is practically coincident with the full spectrum for an ordinary building, allowing the interest of this case study to be extended to the wide building stock erected with obsolete seismic codes or in absence of a correct seismic zonation.

7 Conclusions

This paper presents the results of the vulnerability assessment and the discussion of two retrofitting strategies for a RC strategic building erected around 1990. The case study shows the typical features of a wide class of buildings whose design, fully complying with technical codes, is governed by gravity loads, due to the lack of a correct seismic zonation in the Italian Technical Codes. The resisting system is composed of RC plane frames in the longitudinal direction and erected with a precast construction system in which continuity among beams and columns is achieved through integrative on site casting, and of two eccentric cores. As a first conclusion, the vulnerability assessment permitted to understand the seismic response of the building in its original state, highlighting the building torsional deformability, the role played by frames and core walls and the lack of seismic capacity at element level. Two retrofitting strategies were then discussed, both respecting the constraint of minimizing the interruption of the normal activities in the building and not modifying the original plans, two vital needs for both strategic and ordinary buildings. The stiffening strategy, in which all the resisting elements are classified as primary and can fully exploit their capacity, showed itself to be the only capable of eliminating the torsional deformability, reducing the building deformability and, associated to a local strengthening intervention trough the CAM® system, to provide the required strength to all elements but three walls within the cores.

The results of the analyses provide clear indications for further studies on the stiffening strategy. For the case study, an on-site survey, taking advantage of the standardization of the precast system, could eliminate the strength reduction deriving from incomplete knowledge, and provide the details of beam-to-column joints and especially of the critical connection of the wall W5 to the adjacent beams. A possible difference, while not modifying the global behaviour, could influence significantly the state of stress of the core. As a general conclusion, it appears that investing resources in the level of knowledge can favour the reduction of the retrofitting intervention. As in this case, on site survey can be driven by the preliminary results of response spectrum and pushover analysis. The available ductility in the retrofitted configuration can be assessed through a pushover and can be increased with ad-hoc interventions: as the *q*-factor increases with increasing ductility, the seismic demand decreases. The case study here presented provides an excellent benchmark to investigate on retrofitting strategies, not analyzed here, aiming to provide ductility and energy dissipation to the structure.

Data Availability Statement

Finite Element Models that support the findings of this study are available from the corresponding Author upon reasonable request.

Acknowledgments

This work is based on the MS thesis of L. Stroffolini under the guidance of M.G. Mulas. The support of EDIL CAM® SISTEMI SrL to the second Author during the thesis work is gratefully acknowledged.

References

ASCE-41 (2017) Seismic Evaluation and Retrofit of Existing Buildings (41-17).

Calvi, G.M. (2013) Choices and criteria for seismic strengthening. Journal of Earthquake Engineering, 17 (6), 769-802. https://doi.org/10.1080/13632469.2013.781556

Circ. 2019 (2019) Istruzioni per l'applicazione dell'aggiornamento delle norme tecniche per le costruzioni di cui al decreto ministeriale 17 Gennaio 2018. Circolare n. 7 del 21-01-2019. Gazzetta Ufficiale Serie Generale n.35 del 11-02-2019 - Suppl. Ordinario n. 5 (in Italian).

Choi, E., Chung, Y.-S., Park, J., Cho, B.-S. (2010) Behavior of reinforced concrete columns confined by new steel-jacketing method. ACI Structural Journal, 107 (6), 654-662.

Del Zoppo, M., Di Ludovico, M., Balsamo, A., Prota, A., Manfredi, G. (2017) FRP for seismic strengthening of shear controlled RC columns: Experience from earthquakes and experimental analysis. Composites Part B: Engineering, 129, 47-57. https://doi.org/10.1016/j.compositesb.2017.07.028

EN 1990:2002+A1:2005 (2005) Basis of structural design. European Committee for Standardization (CEN), Brussels

EN 1998-1:2004 (2004) Eurocode 8: Design of structures for earthquake resistance — Part 1: General rules, seismic actions and rules for buildings. European Committee for Standardization (CEN), Brussels

EN 1998-3:2005 (2005) Eurocode 8: Design of structures for earthquake resistance - Part 3: Assessment and retrofitting of buildings. European Committee for Standardization (CEN), Brussels

Karayannis, C.G., Naoum, M.C. (2018) Torsional behavior of multistory RC frame structures due to asymmetric seismic interaction. Engineering Structures, 163, 93-111. https://doi.org/10.1016/j.engstruct.2018.02.038

Kunnath, S.K. (2005) Performance-Based Seismic Design and Evaluation of Building Structures Ch. 5 of Earthquake Engineering for Structural Design, Chen, W. (Ed.), Lui, E. (Ed.). Boca Raton: CRC Press, https://doi.org/10.1201/9781420037142

Ilki, A., Peker, O., Karamuk, E., Demir, C., Kumbasar, N. (2008) FRP retrofit of low and medium strength circular and rectangular reinforced concrete columns. Journal of Materials in Civil Engineering, 20 (2), 169-188. https://doi.org/10.1061/(ASCE)0899-1561(2008)20:2(169)

Mander, J. B., Priestley M. J. N., Park R. (1988) Theoretical stress-strain model for confined concrete. Journal of Structural Engineering, 114(8), 1804–1826. https://doi.org/10.1061/(ASCE)0733-9445(1988)114:8(1804)

Marnetto, R., Leonori, M., Vari, A., (2018) Conservare l'edilizia in muratura - Il Sistema CAM®: Consolidamento strutturale con cuciture INOX. 21mo SECOLO, Guidonia (in Italian).

Mazza, F. (2015) Comparative study of the seismic response of RC framed buildings retrofitted using modern techniques. Earthquake and Structures, 9 (1), 29-48. https://doi.org/10.12989/eas.2015.9.1.029

Monti G., Vailati M., Marnetto R. (2016) Base Isolation and Translation of a Strategic Building Under a Preservation Order. In: D'Amico S. (eds) Earthquakes and Their Impact on Society. Springer Natural Hazards. Springer, Cham. https://doi.org/10.1007/978-3-319-21753-6_16

Mulas, M.G., Perotti, F., Coronelli, D., Martinelli, L., Paolucci, R. (2013) The partial collapse of "Casa dello Studente" during L'Aquila 2009 earthquake. Engineering Failure Analysis, Vol. 34, 566-584.

Mulas, M.G., Martinelli, P. (2017) Numerical Simulation of the Partial Seismic Collapse of a 1960s RC Building. Journal of Performance of Constructed Facilities, 31(6), 04017111. https://doi.org/10.1061/(ASCE)CF.1943-5509.0001102

NTC 2008 (2008) Nuove norme tecniche per le costruzioni. Decreto del Ministro delle Infrastrutture del 14 gennaio 2008. Gazzetta Ufficiale Serie Generale n.29 del 04-02-2008 (in Italian).

NTC 2018 (2018) Aggiornamento delle norme tecniche per le costruzioni. Decreto del Ministro delle Infrastrutture del 17 gennaio 2018. Gazzetta Ufficiale Serie Generale n. 42 del 20-02-2018 (in Italian).

Nuti, C., Bergami, A. (2010) Adeguamento di strutture esistenti in zona sismica: Adeguamento di edifici esistenti. Associazione AICAP.

OPCM 3274 (2003) Ordinanza del Presidente del Consiglio dei Ministri n. 3274. "Primi elementi in materia di criteri generali perla classificazione sismica del territorio nazionale e di normative tecniche per le costruzioni in zona sismica". 20 marzo 2003, Gazzetta Ufficiale n. 105, 8 maggio 2003 (in Italian).

Perrone, D., Aiello, M.A., Pecce, M., Rossi, F. (2015) Rapid visual screening for seismic evaluation of RC hospital buildings. Structures, 3, 57-70. https://doi.org/10.1016/j.istruc.2015.03.002

Ruggieri, S., Perrone, D., Leone, M., Uva, G., Aiello, M.A. (2020) A prioritization RVS methodology for the seismic risk assessment of RC school buildings. International Journal of Disaster Risk Reduction, 51, art. no. 101807. https://doi.org/10.1016/j.ijdrr.2020.101807

Ruggieri, S., Porco, F., Uva, G., Vamvatsikos, D. (2021) Two frugal options to assess class fragility and seismic safety for low-rise reinforced concrete school buildings in Southern Italy. Bulletin of Earthquake Engineering, 19 (3), 1415-1439. https://doi.org/10.1007/s10518-020-01033-5

SAP2000 (2018) Computers and Structures, Version 20.2.0.

Thermou, G.E., Elnashai, A.S. (2006) Seismic retrofit schemes for RC structures and local-global consequences. Progress in Structural Engineering and Materials, 8 (1), 1-15. https://doi.org/10.1002/pse.208

Thermou, G.E., Psaltakis, M. (2018) Retrofit Design Methodology for Substandard R.C. Buildings with Torsional Sensitivity. Journal of Earthquake Engineering, 22 (7), 1233-1258. https://doi.org/10.1080/13632469.2016.1277569

Xiao, Y., Wu, H. (2003) Retrofit of reinforced concrete columns using partially stiffened steel jackets. Journal of Structural Engineering, 129 (6), 725-732. https://doi.org/10.1061/(ASCE)0733-9445(2003)129:6(725)

Zerbin, M., Aprile, A. (2015) Sustainable retrofit design of RC frames evaluated for different seismic demand. Earthquake and Structures, 9 (6), 1337-1353. https://doi.org/10.12989/eas.2015.9.6.1337

Appendix

Table A1 – Dimensions and reinforcement ratios of columns cross-section, building B1. Section numbers in bold denotes cross-section having a higher stiffness in the transverse (out-of-plane) direction.

Ground floor	**Section [cm]**		**ρ_s [%]**
	b_X	**b_Y**	
C.1.1	40	25	0.80
C.1.2	40	40	0.95
C.1.3	40	40	0.95
C.1.4	40	40	0.95
C.1.5	40	40	0.95
C.1.6	40	40	0.95
C.1.7	40	40	0.79
C.1.8	40	**50**	0.76
C.1.9	40	**50**	1.41
C.1.10	40	**50**	1.41
C.1.11	50	50	0.88
C.1.12	50	50	0.88
C.1.13	50	50	0.88
C.1.14	40	**50**	1.41
C.1.15	40	30	0.85
C.1.16	40	30	1.05
C.1.17	40	**50**	1.06
C.1.18	40	**50**	1.06
C.1.19	40	**50**	1.06
C.1.20	40	40	0.95

First floor	**Section [cm]**		**ρ_s [%]**
	b_X	**b_Y**	
C.2.1	40	25	0.80
C.2.2	40	30	1.05
C.2.3	40	30	1.05
C.2.4	40	30	1.05
C.2.5	40	30	1.05
C.2.6	40	30	1.05
C.2.7	40	40	0.79
C.2.8	40	40	0.79
C.2.9	40	40	0.95
C.2.10	40	40	0.95
C.2.11	40	**50**	0.90
C.2.12	40	**50**	0.90
C.2.13	40	**50**	0.90
C.2.14	40	**50**	1.41
C.2.15	40	25	1.02
C.2.16	40	30	1.05
C.2.17	40	40	0.79
C.2.18	40	40	0.79
C.2.19	40	40	0.79
C.2.20	40	40	0.95

Second floor	**Section [cm]**		**ρ_s [%]**
	b_X	**b_Y**	
C.3.1	40	25	0.62
C.3.2	40	30	0.85
C.3.3	40	30	0.85
C.3.4	40	30	0.85
C.3.5	40	30	0.85
C.3.6	40	30	0.85
C.3.7	40	30	1.05
C.3.8	40	30	0.85
C.3.9	40	30	0.85
C.3.10	40	30	0.85
C.3.11	40	40	0.79
C.3.12	40	40	0.79
C.3.13	40	40	0.79
C.3.14	40	40	0.95
C.3.15	40	25	0.80
C.3.16	40	30	1.05
C.3.17	40	30	0.85
C.3.18	40	30	0.85
C.3.19	40	30	0.85
C.3.20	40	40	0.79

Third floor	**Section [cm]**		**ρ_s [%]**
	b_X	**b_Y**	
C.4.1	40	25	0.62
C.4.2	40	30	0.67
C.4.3	40	30	0.67
C.4.4	40	30	0.67
C.4.5	40	30	0.67
C.4.6	40	30	0.67
C.4.7	40	30	1.05
C.4.8	40	25	0.80
C.4.9	40	25	0.62
C.4.10	40	25	0.62
C.4.11	40	30	0.67
C.4.12	40	30	0.67
C.4.13	40	30	0.67
C.4.14	40	40	0.95
C.4.15	40	25	0.62
C.4.16	40	30	1.05
C.4.17	40	30	0.67
C.4.18	40	30	0.67
C.4.19	40	30	0.67
C.4.20	40	30	1.05